ISSN 0030-400X, Optics and Spectroscopy, 2015, Vol. 118, No. 6, pp. 930–935. © Pleiades Publishing, Ltd., 2015.

CONDENSED-MATTER SPECTROSCOPY

Absorption Enhancement in Thin-film Photoluminescence Layers with Metal Nanoparticles Inter-coupling Engineering[1]

Sajjad Yadollahzadeh[a], Saba Alavizadeh[c], and Hamed Baghban[b]

[a] *Young Researchers and Elite Club, Tabriz Branch, Islamic Azad University, Tabriz, Iran*

[b] *School of Engineering-Emerging Technologies, University of Tabriz, Tabriz 5166614761, Iran*

[c] *Pardis International Campus, University of Tabriz, Tabriz, Iran*

e-mail: s.yadollahzadeh@gmail.com

Received November 14, 2014

Abstract—We analyze the enhancement in optical absorption of a photoluminescence ZnS layer with embedded spherical metal nanoparticles (MNPs). Using introduced optical model based on the boundary element method (BEM), the so-called scattering cross-section over absorption cross-section (SCS/ACS) ratio has been defined that represents the strength of re-absorption by scattering. According to the collective behavior of the interacting plasmonic nanoparticles in an array, an optimum SCS/ACS is obtained for inter-particle distance over the particle diameter. This parameter gives a hint for the nanoparticle density and size in practical applications and is consistent for all of the metallic nanoparticles.

DOI: 10.1134/S0030400X15060181

INTRODUCTION

Luminescence intensity enhancement process of fluorophores by coupling with localized surface plasmons (SP) of metallic nanostructures offers promise for a range of applications including light-emitting diodes, electro- and photoluminescence (EL and PL) devices, and biosensors [1–3].

Two possible mechanisms of PL/electroluminescence enhancement including metal-enhanced fluorescence and exciton energy transfer have been reported. In the later process, the exciton energies are transferred into surface plasmon modes of the metallic nanoparticles while in the former mechanism, enhancement of light absorption as well as radiative and nonradiative decay in fluorophores, are modified by the interaction with nearby plasmonic nanostructures. These characteristics of plasmonic excitations strongly depend on particle geometry, size, and density, and give rise to different effects, such as frequency-dependent absorption and scattering or near field enhancement.

In photovoltaic devices, the combination of metal nanopartieles (MNPs) and semiconductor materials is intended to enhance the absorption in absorber layers, due to plasmonic scattering enabling their thickness reduction which yields new possibilities for the design of luminescence layer, thin film solar cells and photodetectors [4, 5]. For optical photodetectors, the device performance could be improved via the plasmonic effect induced by MNPs without increasing the area of the active region which makes it possible to increase photodetector responsivity without sacrificing device speed [5]. Also, an efficient PL device can benefit from a broad and strong absorption spectrum and absorption coefficient for all parts of exciting light.

Although numerous researches have been performed on optical specifications of photodetector, photovoltaic, and EL devices in the presence of plasmonic nanoparticles, the field of PL devices has not received that much attention yet. Also, there are few reports considering back reflection from MNPs and therefore, only the apparent increase in PL enhancement has been considered without separating the effects by the SP resonance and light scattering which results in prolonged optical-path length [6].

Here we address the absorption enhancement management in ZnS thin film which is one of mostly used host materials for PL devices both in the film and nanoparticle form [7]. Intense emission from ZnS layer not only is used for solid state lighting but also offers a very sensitive method for radiation detection [8]. Hence, the importance of excitation enhancement in PL layers is highlighted. The presented approach involves an optical model that combines scattering and absorption from coupled MNPs with the propagation of light in host ZnS layer. Regardless of the PL layer excitation enhancement managing by different nanoparticles, the introduced model gives an insight into plasmonic nanoparticle size and density in variety of optoelectronic devices such as solar cells and pho-

[1] The article is published in the original.

todetectors at different light spectrum regions based on the so-called scattering cross-section over absorption cross-section ratio.

So far, modeling of MNPs has addressed aspects of particle composition [9], size, shape and dielectric environment [10–12]. In the dipolar limit, the plasmonic resonance wavelength is completely determined by the particle shape. However, for a certain particle shape, as the particle diameter is increased, the results considerably differ from the limiting electrostatic curve obtained in the dipole approximation. Beside the optics of individual plasmonic nanoparticles, the collective behavior of the interacting plasmonic nanoparticles is of great interest for optoelectronic applications.

Various analytical and numerical methods have been introduced to solve the Maxwells equations to obtain the SCS and ACS of dielectric and metal nanoparticles. The most popular and simple analytical introduced method is the dipole approximation [13]. However, developed theoretical methods are required which are not limited to composition and geometrical condition due to rapid progress in demonstration of plasmonic nanostructures in the recent years. The classical Mie approach [10] also formulates light scattering and absorption by a spherical particle embedded in a homogeneous non-absorbing medium. However, to evaluate the optical absorption of an absorbing host medium, a generalization is necessary.

Particularly, the finite difference time domain (FDTD) [14], the discrete dipole approximation (DDA) [15], the finite element method (FEM) [16], the multiple multipole method [10], the Method of Moments (MoM), or the multiple scattering method [17] are some of the most famous numerical methods. BEM is another solution method which presents results with considerably good agreement with experimental data. The BEM is specially a suitable approach for homogeneous and isotropic dielectric environments, where the embedded bodies are separated by sharp boundaries [18]. In the following, at first the BEM is described in short and later, the obtained results will be discussed for Al, Ag, and Au metal nanoparticles. The analysis of the features of coupled MNPs includes the investigation of various structures such as 1D chain and 2D array (clusters of spherical particles on a substrate) in our study.

THEORETICAL BACKGROUND

Figure 1 illustrates a scheme of MNPs-embedded ZnS film which is under the illumination for excitation. Upon exciting the MNPs with an incident electromagnetic radiation, nanoparticles become polarized. Nanoparticles have been considered in our model through local and isotropic dielectric functions $\varepsilon_j(\omega)$ which are separated by sharp boundaries, ∂V_j. Also, Maxwell's equations are assumed in frequency

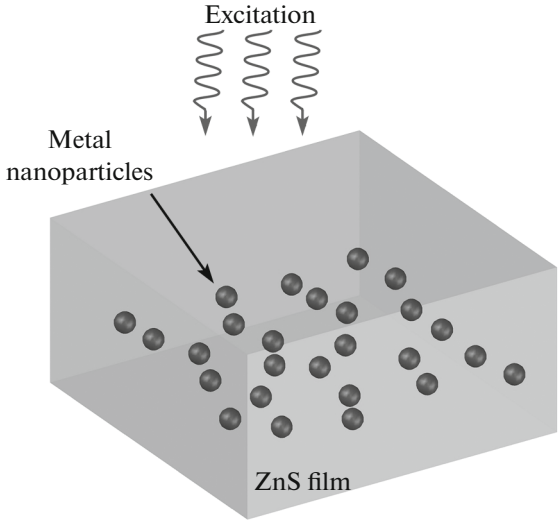

Fig. 1. Metallic nanoparticles embedded in a PL ZnS layer.

space ω, and the magnetic permeability is set to $\mu = 1$ [12]. The well-known scalar and vector potentials $\phi(r)$ and $A(r)$ are related to the electromagnetic fields with the following relations

$$E = ikA - \nabla\phi, \quad B = \nabla \times A, \tag{1}$$

$$k = \omega/c, \quad \nabla A = ik\varepsilon\phi, \tag{2}$$

where k, c are the wave number and speed of light in vacuum, respectively. Green function is then set for the Helmholtz equation through

$$(\nabla^2 + k_j^2)G_j(r,r') = -4\pi\delta(r-r'),$$
$$G_j(r,r') = \frac{e^{ik_j|r-r'|}}{|r-r'|}, \tag{3}$$

$$k_j = \sqrt{\varepsilon_j}k, \quad r \in V_j. \tag{4}$$

The scalar and the vector potentials can be rewritten according to the introduced Green function as

$$\phi(r) = \phi_{\text{ext}}(r) + \oint_{V_j} G_j(r,s)\sigma_j(s)ds, \tag{5}$$

$$A(r) = A_{\text{ext}}(r) + \oint_{V_j} G_j(r,s)h_j(s)ds. \tag{6}$$

This $\sigma_j, h_j, \phi_{\text{ext}}$, and A_{ext} are surface charge, current distributions, the scalar and vector potentials characterizing the external perturbation, respectively in the above relations. Based on the introduced potentials, the absorption, scattering and extinction cross sections of the MNPs will be obtained as follows [12]:

$$C_{\text{sca}} = n_b \oint_{\partial\Omega} \text{Re}\{\hat{n}(E \times B^*)\}da, \tag{7}$$

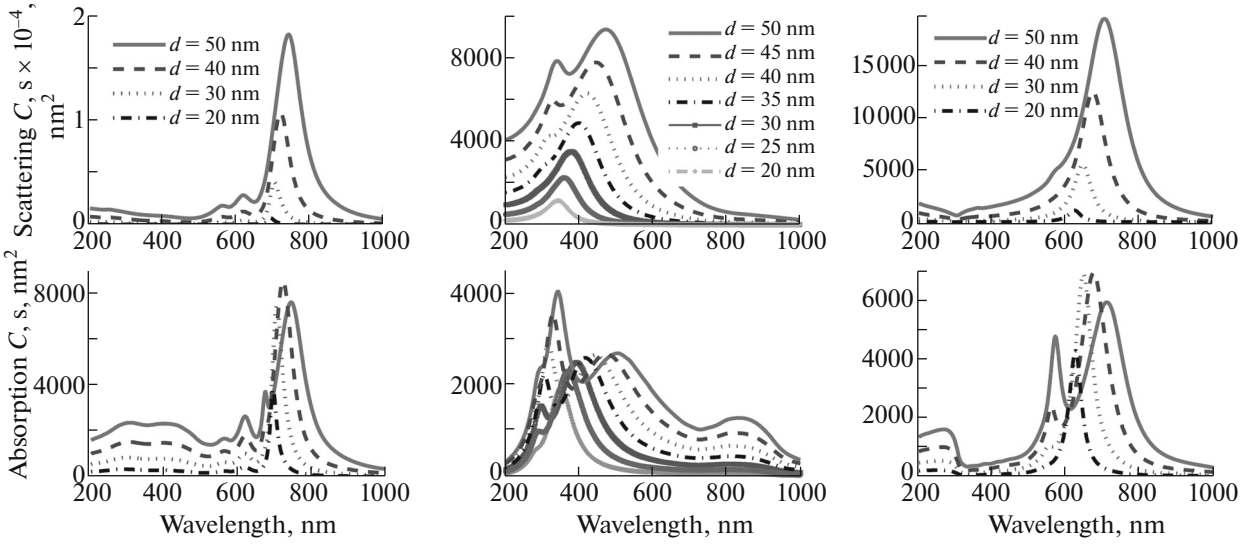

Fig. 2. Absorption and scattering spectra for Au, Al, and Ag metallic spheres (from left to right, respectively) in ZnS host with corresponding particle diameter as study parameter.

$$C_{\text{ext}} = -\frac{1}{n_b}\oint_{\partial\Omega} \text{Re}\{\hat{n}(E \times B^*_{\text{inc}} + E^*_{\text{inc}} \times B)\}da, \quad (8)$$

$$C_{\text{abs}} = C_{\text{ext}} - C_{\text{sca}}, \quad (9)$$

where $n_b, \hat{n}, E_{\text{inc}}, B_{\text{inc}}$, and $\partial\Omega$ are the background refractive index, unit vector in the direction of the scattering, the electric field and magnetic field of the incident plane wave, and the surface area, respectively. The transmitted light intensity through the film with a density of $N(m^{-3})$ of embedded 15 nm radius MNPs and thickness H is obtained as follows:

$$I = I_0 \exp[-\alpha_0\left(1 - \frac{4}{3}\pi r^3 N\right) - (C_{\text{abs}} + C_{\text{sca}})N]H, \quad (10)$$

where

$$I = I_0 \exp\left[-\alpha_0\left(1 - \frac{4}{3}\pi r^3 N\right)\right]H$$

defines the power absorption by host material excluding the volume occupied by the MNPs and

$$I = I_0 \exp[(C_{\text{abs}} + C_{\text{sca}})N]H$$

corresponds to the absorption by the MNPs and the scattered power by the MNPs, which will be re-absorbed by the host material. The fraction

$$\left[\alpha_0\left(1 - \frac{4}{3}\pi r^3 N\right) + C_{\text{sca}}N\right] / \left[\alpha_0\left(1 - \frac{4}{3}\pi r^3 N\right) + (C_{\text{abs}} + C_{\text{sca}})N\right]$$

of absorbed power indicates the absorption in the host material.

Figure 2 shows the absorption and scattering spectra calculated by BEM theory for Au, Al, and Ag MNPs in the host ZnS with the particle diameter d considered as study parameter. A broadening and also red shift occurs in the spectra with increasing the particle diameter. This behavior can be utilized for fast and moderate particle sizing [19]. Also, the resonance shift is negligible for smaller particles, while the broadening is completely obvious due to surface electron scattering and size-limiting effects [20].

To gain better insight into the mechanisms which determine the effect of inter-particle coupling on the optical cross section of the host photoluminescence layer, the absorption and scattering spectra for a linear chain and 2D square array of Ag, Al, and Au nanoparticles has been calculated using the BEM method with particle diameters of $d = 30$ nm separated by a variable distance denoted by s and the results are presented in Figs. 3, 4 and 5 for a linear chain (left column) and 2D square array (right column) of Ag, Al, and Au nanoparticles, respectively. In this case, the incident TE and TM waves have been assumed to be perpendicular to cluster axis or plane. For the linear chain, TM polarization corresponds to electric vector along the chain axis, while for 2D array, the TM and TE polarizations are equivalent. As the results indicate, when the inter-particle separation satisfies the condition $s/d \geq 0.5$, the absorption and scattering efficiencies approach the single-particle quantities. However, when the relative distance s/d, is about several percent the situation changes severely and the obtained spectra due to coupled NPs reveals obvious branching into two components with highlighted red-shifting of the long-wavelength resonance when the spheres approach each other.

Generally, there are two characteristic absorption peaks for the linear chain where the short wavelength

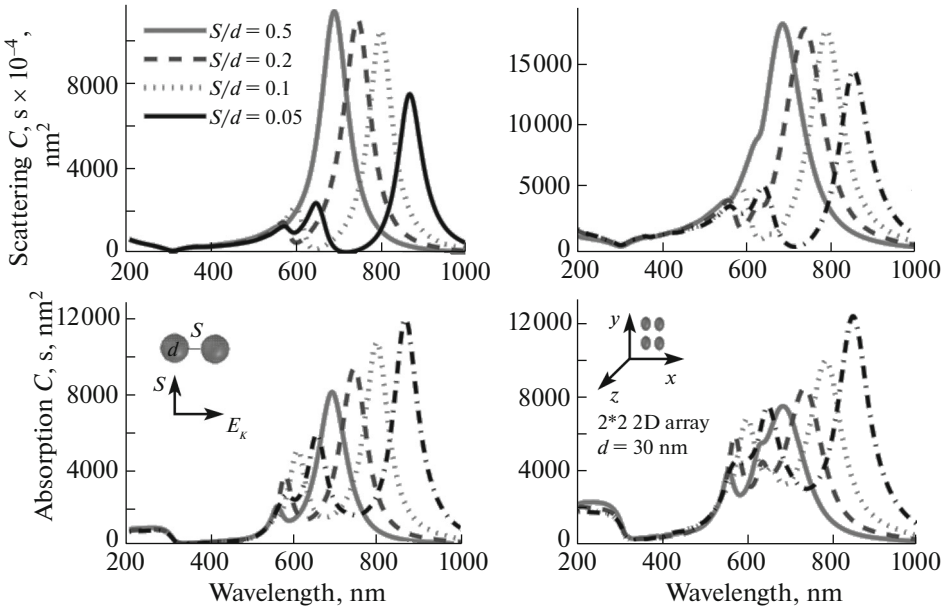

Fig. 3. Absorption and scattering spectra of linear chains and 2D square array of Ag metallic spheres in ZnS host. The particle diameter is 30 nm and particles are separated by a variable distance, s (s/d parameter denotes the inter-particle distance over the particle diameter).

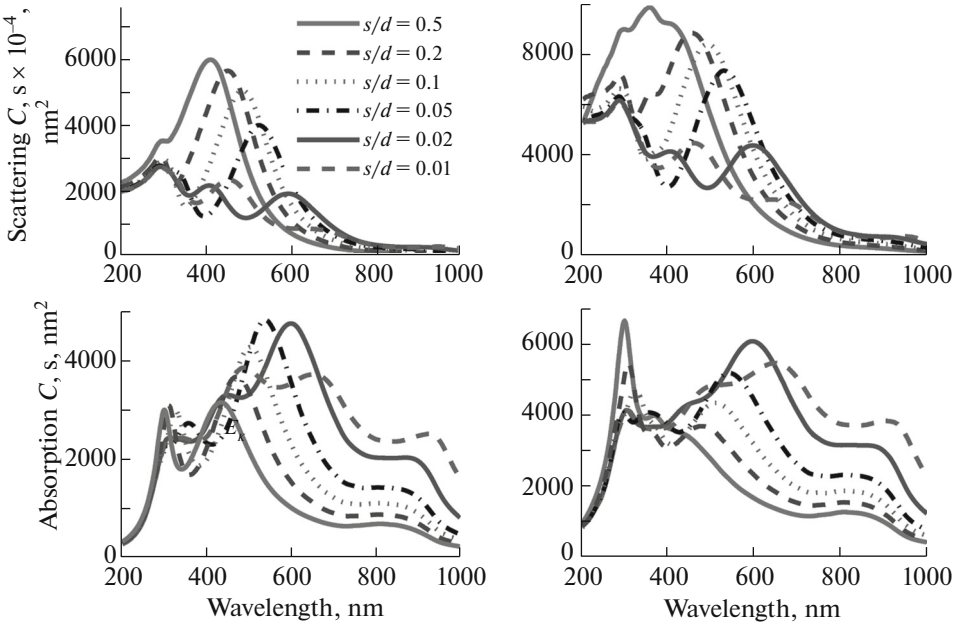

Fig. 4. Absorption and scattering spectra of linear chains and 2D square array of Al metallic spheres in ZnS host. The particle diameter is 30 nm and particles are separated by a variable distance, s (s/d parameter denotes the inter-particle distance over the particle diameter).

peak corresponds to the plasmonic resonance of individual nanoparticles which are excited with TE mode while the long-wavelength resonance appears at the electric axial chain excitation which is regarded to strong electrodynamic coupling of chain spheres.

For unpolarized illumination, both modes are obvious in the spectra. The metal clusters with low and high particle densities are two important cases that should be considered. Excitation of each particle in the cluster by the incident illumination and the scat-

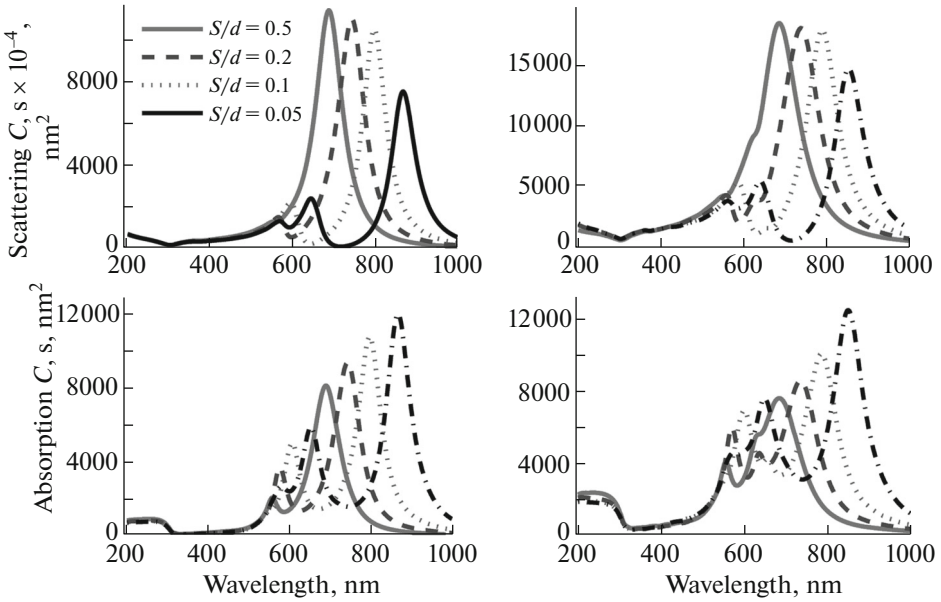

Fig. 5. Absorption and scattering spectra of linear chains and 2D square arrays of Au metallic spheres in ZnS host. The particle diameter is 30 nm and particles are separated by a variable distance, s (s/d parameter denotes the inter-particle distance over the particle diameter).

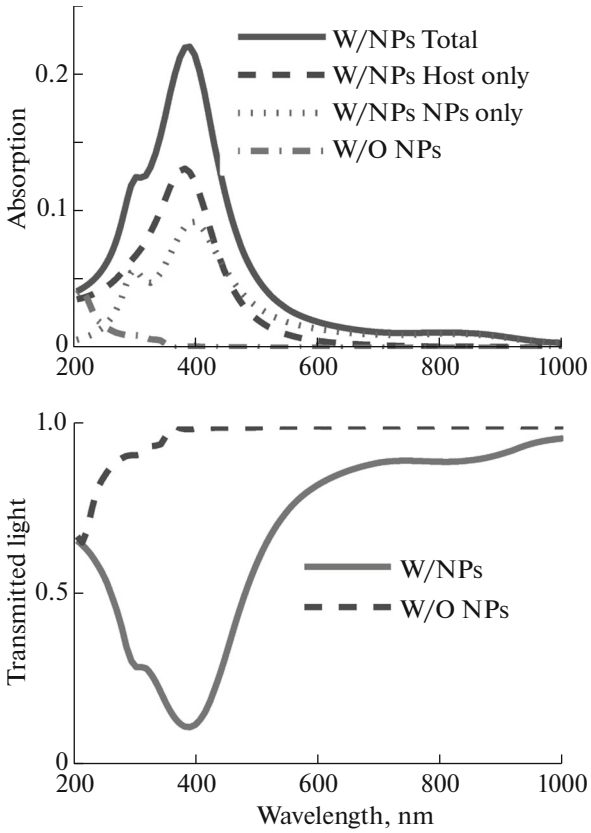

Fig. 6. (top) Absorption in Al MNPs (dotted curve) and ZnS host material (dashed curve) for MNP concentration of $1/(30\ \text{nm})^3$ and 10 nm film thickness. The total absorption (solid curve) and absorption for the case of a homogeneous ZnS film (dash-dotted curve) are also shown. (bottom) The total transmitted light with NPs (solid curve) and for the case of a homogeneous ZnS film without NPs (dashed curve).

tering waves from other excited particles have been considered in the first case. The far-field scattering properties of a cluster are determined by interference of all multiple scattered far field waves. Accordingly, there are no significant differences between multiple scattering from dielectric and metallic clusters, provided that all particles are separated by a distance larger than their size. However, for densely packed aggregates, the situation is quite different. The single particle near-field strongly interact with the field of other particles for metal NPs close to each other with separation distance less than ~0.1 NP size which results in variation of the total spectrum.

Results for a chain of MNPs show that for larger particles the extinction spectra reveal multiple peaks (e.g. quadrupole peaks for a chain of four-in-row MNPs) and significant contribution of scattering.

It is clear from comparing the scattering and absorption cross sections curves that Al nanoparticles exhibit higher scattering cross section in the UV range which is much appropriate for ZnS thin films with a wide and direct band gap of Eg, bulk = 3.6 eV. Although the ratio of SCS/ACS varies at different excitation wavelengths for linear chain and square array of Al nanoparticles (Fig. 6), an optimum SCS/ACS is obtained for $s/d = 0.5$. This parameter gives a hint for the nanoparticle density and size for practical investigations and is even consistent for optimum SCS/ACs value for both the Ag and Au nanoparticles. As depicted in Fig. 6, absorption in Al MNPs and ZnS host material for MNP concentration of $1/(30\ \text{nm})^3$ and 10 nm film thickness have been compared and the total transmitted light for the host

layer in the presence and without the MNPs have been obtained. Also, efficient PL observed from the ZnS QDs excited by two-photon absorption in near-infrared window (NIR-I: 650–950 nm and NIR-II: 1000–1350 nm) [21], can be further enhanced by Ag and Au nanoparticles with optimum SCS/ACs value in the obtained wavelength region.

CONCLUSION

Based on BEM, the SCS/ACS quantity was introduced in this article as a factor for comparing the absorption enhancement of PL ZnS layer in the presence of Ag, Au, and Al nanoparticles. According to the collective behavior of the interacting plasmonic nanoparticles in a linear chain or a square array, an optimum SCS/ACS was obtained and it was shown that inter-particle coupling red-shifts the extinction cross section of the MNPs and broadens the extinction spectra. The exciting spectra therefore can be managed to obtain desired absorption range. Regardless of efficient excitation enhancement by Al nanoparticles considering the ZnS band gap, this study gives a thumb rule for plasmonic nanoparticle size and density for different metallic nanoparticles in variety of optoelectronic devices such as solar cells and photodetectors at different light spectrum since the results are consistent for different nanoparticles at wide wavelength range based on the introduced SCS/ACS factor. Results of this study can be utilized to obtain intense PL from ZnS layer for solid state lighting considering that the excitation light may lie at UV range or near-infrared windows utilizing multi-photon absorption process.

ACKNOWLEDGMENTS

We would like to thank Prof. Nikolai G. Khlebtsov for his valuable works in the field of plasmonic nanoparticles.

REFERENCES

1. P. Pompa, L. Martiradonna, A. Della Torre, F. Della Sala, L. Manna, M. De Vittorio, F. Calabi, R. Cingolani, and R. Rinaldi, Nature Nanotechnol. **1** (2), 126 (2006).
2. A. Fujiki, T. Uemura, N. Zettsu, M. Akai-Kasaya, A. Saito, and Y. Kuwahara, Appl. Phys. Lett. **96** (4), 043307 (2010).
3. K. Aslan, I. Gryczynski, J. Malicka, E. Matveeva, J. R. Lakowicz, and C. D. Geddes, Curr. Opin. Biotechnol. **16** (1), 55 (2005).
4. J.-Y. Lee and P. Peumans, Opt. Express. **18** (10), 10078 (2010).
5. T. Ishi, J. Fujikata, K. Makita, T. Baba, and K. Ohashi, Japan. J. Appl. Phys. **44** (3L), L364 (2005).
6. D.-R. Jung, J. Kim, C. Nahm, S. Nam, J. I. Kim, and B. Park, Mater. Res. Bull. **47** (2), 453 (2012).
7. J. S. McCloy and B. G. Potter, Opt. Mater. Express **3** (9), 1273 (2013).
8. L. Ma, K. Jiang, X.-T. Liu, and W. Chen, J. Appl. Phys. **115** (10), 103104 (2014).
9. N. G. Khlebtsov, Quant. Electron. **38** (6), 504 (2008).
10. L. Novotny and B. Hecht, *Principles of Nano-Optics* (Cambridge Univ. Press, 2012).
11. F. G. De Abajo, Rev. Mod. Phys. **82** (1), 209 (2010).
12. J. D. Jackson and J. D. Jackson, *Classical Electrodynamics* (Wiley, New York, 1962).
13. C. F. Bohren and D. R. Huffman, *Absorption and Scattering of Light by Small Particles* (Wiley, New York, 2008).
14. A. Taflove and S. C. Hagness (2000).
15. M. A. Yurkin, D. De Kanter, and A. G. Hoekstra, J. Nanophoton. **4** (1), 041585 (2010).
16. J. Jin, *The Finite Element Method in Electromagnetics* (Wiley, 2014).
17. N. G. Khlebtsov, J. Quant. Spectrosc. Radiat. Transfer **123,** 184 (2013).
18. A. Sutradhar, G. H. Paulino, and L. J. Gray, *Symmetric Galerkin Boundary Element Method* (Springer, 2008).
19. W. Haiss, N. T. Thanh, J. Aveyard, and D. G. Fernig,Anal. Chem. **79** (11), 4215 (2007).
20. N. G. Khlebtsov and L. A. Dykman, J. Quant. Spectrosc. Radiat. Transfer **111** (1), 1 (2010).
21. R. Subha, V. Nalla, J. H. Yu, S. W. Jun, K. Shin, T. Hyeon, C. Vijayan, and W. Ji, J. Phys. Chem. C **117** (40), 20905 (2013).